Tricritical Ising phase transition in a two-ladder Majorana fermion lattice

Xiaoyu Zhu[1,2] and M. Franz[2]

[1]*National Laboratory of Solid State Microstructures and Department of Physics, Nanjing University, Nanjing 210093, China*

[2]*Department of Physics and Astronomy and Quantum Matter Institute, University of British Columbia, Vancouver, British Columbia, Canada V6T 1Z4*

We introduce a two-ladder lattice model with interacting Majorana fermions that could be realized on the surfaces of a topological insulator film. We study this model with a combination of analytical and numerical techniques, and we find a phase diagram that features both gapless and gapped phases as well as interesting phase transitions including a quantum critical point in the tricritical Ising (TCI) universality class. The latter occurs at an intermediate-coupling strength at a meeting point of a first-order transition line and an Ising critical line, and it is known to be described by a superconformal field theory with central charge $c = \frac{7}{10}$. We discuss the experimental feasibility of constructing the model and tuning parameters to the vicinity of the TCI point where signatures of the elusive supersymmetry can be observed.

I. INTRODUCTION

The tricritical Ising (TCI) phase transition occurs when an Ising phase-transition line meets a first-order transition line. At this critical point, three different phases become indistinguishable. The critical exponents also experience a dramatic change when the system goes from the Ising critical line to the TCI point as the latter belongs to a different universality class [1]. In conformal field theory (CFT) language, TCI CFT is the second unitary minimal model, with central charge $c = \frac{7}{10}$, whereas the Ising CFT has $c = \frac{1}{2}$ [2]. Recent interest in the physical realizations of TCI CFT stems from the fact that it is the simplest known CFT that exhibits supersymmetry, a special type of symmetry that interchanges bosonic and fermionic fields. This enigmatic property has been conjectured to cure many problems in high-energy physics but remains experimentally unobserved [3]. Technically, the TCI point can be described by a superconformal field theory [4–6], which is developed by extending the Virasoro algebra in CFT to its supersymmetric counterpart.

There are two well-known spin models in the literature that realize TCI CFT: the Blume-Capel model [7,8] and the Ising metamagnet model [9]. The former is a modified Ising model where each spin site is allowed to be vacant. The latter is an Ising antiferromagnetic model with next-nearest-neighbor ferromagnetic interaction. Despite extensive searches, TCI quantum criticality and the associated supersymmetry have yet to be observed experimentally in spin models. Other condensed-matter systems have therefore been considered recently as potential platforms for the observation of TCI points and the associated supersymmetry. Among these, condensed-matter realizations of Majorana fermions—Majorana zero modes (MZMs) [10–14]—lend themselves naturally to this task. As exotic bound states, MZMs were predicted to emerge in topological superconducting systems. While the noninteracting theories of MZMs are now well developed, a lot of interest is currently focused on interaction effects [15–19] as well as understanding the signatures of the interacting regime [20,21]. Going beyond the mean-field description of superconductivity, several proposals were put forward in number-conserving fermionic systems with either attractive or repulsive interactions, where Majorana or Majorana-like bound states were demonstrated to occur at the boundaries [22–24]. Here, instead of studying how interactions influence the formation of individual MZMs, we consider interaction effects in a Majorana fermion lattice where each site consists of a single MZM.

It is well known that a simple noninteracting one-dimensional (1D) chain of MZMs (a critical Kitaev chain) maps onto the transverse field Ising model tuned to its critical point and realizes a $c = \frac{1}{2}$ CFT [25]. Breaking the translation symmetry through dimerization produces various gapped phases [26], while coupling MZMs to bosonic modes [27] or adding four-fermion interactions [28,29] has been shown to give rise to TCI behavior with $c = \frac{7}{10}$ by tuning a single model parameter. As the evidence supporting the existence of MZMs in condensed-matter systems has been growing [30–35], the possibility of realizing the TCI criticality built upon this platform is becoming more promising. With the rapid development in this field, one can expect in the near future to manipulate MZMs and to be able to engineer interacting lattice models envisioned theoretically [27–29]. At the same time, realization of these models presents significant challenges. The model of Ref. [27] requires Majorana modes to couple to bosonic (spin) modes, and it is not clear how such coupling might be engineered and controlled. The model of Ref. [28] only requires short-range four-fermion interaction, which is generically present in the system, but the TCI point occurs only at very strong coupling.

In the present paper, we construct a fermionic model with short-range four-fermion interactions that is more complex than models of Refs. [27,28] but has an advantage that it exhibits a TCI point at weak to intermediate interaction strength and does not require coupling to bosonic modes. Similar to the spin models [7–9], two parameters must be tuned to reach the TCI point. The model can be realized in the Fu-Kane superconductor [36] that occurs at the interface between a 3D strong topological insulator and an ordinary *s*-wave superconductor. Here MZMs are bound in the cores of Abrikosov vortices and form a periodic lattice in the applied magnetic field. Effective theories for MZMs in such vortex lattices have been studied recently [37–42], with the
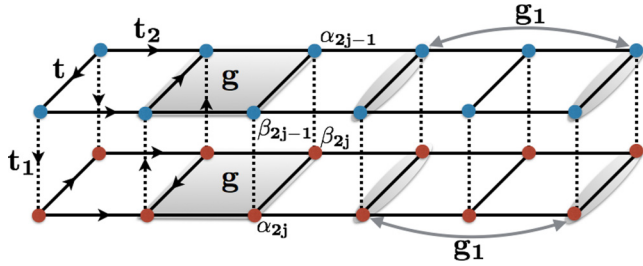
FIG. 1. Geometry of the two-ladder MZM lattice. Blue dots represent vortices, and red dots are antivortices. The arrow is added to indicate the sign of bilinear hopping terms. If the arrow starts from a site denoted by α to β, the bilinear term is written as $i\alpha\beta$. The interaction term g involves four MZMs on the nearest-neighbor rungs while g_1 connects next-nearest-neighbor rungs.

conclusion that they realize a convenient platform to probe interacting phases of Majorana fermions.

II. THE MODEL AND ITS REALIZATION

The model we consider consists of two coupled ladders, each formed out of Majorana sites as schematically depicted in Fig. 1. The upper ladder is composed of vortices, and the lower one of antivortices. Each of them hosts a single MZM. A realistic setup that can realize this model is a thin film of a topological insulator in proximity to superconducting films on the two surfaces. When an external magnetic field perpendicular to the surfaces is applied, vortices and antivortices are induced on the upper and lower surface, respectively. At the so called neutrality point (i.e., when the chemical potential μ of the TI coincides with the Dirac point), the Fu-Kane superconductor in each surface develops an extra chiral symmetry [43], which changes its noninteracting topological classification from $\mathbb{Z}_2$ to $\mathbb{Z}$. The latter implies that the bilinear tunneling terms between MZMs bound in two vortices of the same type are prohibited, while four-fermion interaction terms are allowed and could thus be dominant. There is no restriction on the tunneling terms between a vortex and an antivortex. Slightly away from the neutrality point, tunneling terms between two vortices of the same type are allowed but are generically small. In the two-ladder system, we shall work in the regime where tunneling and interaction terms among vortices of the same type are comparable and the terms involving vortices and antivortices are dominated by tunneling.

If we assume that there are $2N$ MZM sites, then the above discussion leads to the following Hamiltonian for the two-ladder system depicted in Fig. 1,

$$H = \sum_{j=1}^{N/2} (-1)^{j-1} [it(\alpha_{2j}\beta_{2j} + \alpha_{2j-1}\beta_{2j-1})$$

$$+ it_1(\alpha_{2j-1}\beta_{2j} + \beta_{2j-1}\alpha_{2j})] + \sum_{j=1}^{N-4} g_1\alpha_j\beta_j\alpha_{j+4}\beta_{j+4}$$

$$+ \sum_{j=1}^{N-2} [it_2(\alpha_j\alpha_{j+2} + \beta_j\beta_{j+2}) + g\alpha_j\beta_j\alpha_{j+2}\beta_{j+2}]. \quad (1)$$

Here α_j and β_j are MZM operators at site j, with $\{\alpha_j, \alpha_{j'}\} = 2\delta_{j,j'}$, $\{\beta_j, \beta_{j'}\} = 2\delta_{j,j'}$, and $\{\alpha_j, \beta_{j'}\} = 0$. The t_1 term couples MZMs bound in vortices and antivortices, and the remaining terms all involve MZMs bound in the vortices of the same type. The sign of each bilinear term is chosen to satisfy the Grosfeld-Stern rule [44]. Other sign choices are possible in principle, and some of them would support the physics discussed below while others would not. We shall focus here on signs consistent with the Grosfeld-Stern rule and leave other choices to future investigations. Furthermore, we assume g and g_1 to be positive, corresponding to attractive interactions. In principle, the signs of t, t_1, and t_2 can be either positive or negative, but these are equivalent since one can always perform a unitary transformation that changes the sign of only one of them without affecting the others. For instance, to change the sign of t, we simply take $(\alpha, \beta)_j \to (\beta, \alpha)_j$, which has no influence on the energy spectrum. Hence we will only consider the case in which all t's and g's are non-negative. We further note that other tunneling and four-fermion interaction terms are allowed by symmetries in the Hamiltonian (1), but these will not qualitatively change the conclusions reached below as long as their strength is not large.

In general, one needs at least three independent parameters to realize a model capable of supporting a TCI point, and in order to reach the transition two of them need to be fine-tuned. Fermionic models with an extra symmetry [27,28] represent an exception to this rule such that the TCI point is reached by tuning a single parameter. For our specific model, as we will see later, all the terms except t_2 in Eq. (1) are required to induce the TCI phase transition. To make it simple, we begin by setting $t_2 = 0$ for the moment and recover it later to study how TCI points are affected. As mentioned earlier, a TCI point can be thought of as the meeting point of a first-order phase-transition line and an Ising transition line. So the system is required to have both first-order transition points and Ising critical points. The first-order phase transition occurs naturally in our model when $t_1 = 0$. In this case, the two ladders are decoupled and thus we need to only consider one of them. To see where the transition occurs, we perform a unitary transformation $[(\alpha, \beta)_{2j-1} \to (\beta, \alpha)_{2j-1}$ for $j \in$ even] on the upper ladder, and we rewrite the Hamiltonian in terms of Dirac fermion operators $c_j = (\alpha_j + i\beta_j)/2$. We obtain

$$H_u = \sum_{j \in \text{odd}}^{N} 2n_j[t - 2g(1 - n_{j+2}) + 2g_1(1 - n_{j+4})], \quad (2)$$

where $n_j = c_j^\dagger c_j$ is the occupation number operator that takes values either 0 (empty) or 1 (occupied). Note that constant terms are left out in Eq. (2), and a periodic boundary condition, $n_{N+j} = n_j$, is assumed.

Since n_j is a good quantum number in Eq. (2), all the eigenstates of H_u are also eigenstates of n_j, characterized by each site being empty or occupied. It is not difficult to see that the system favors a doubly degenerate ground state when $t < 2g$, with every other site being occupied. For $t > 2g$, the ground state is unique with all sites empty. Evidently, the ground state experiences an abrupt change when the system passes the transition point at $t = 2g$. In addition, when $g_1 > 0$ the system at the transition point exhibits a finite gap $\Delta = 4g_1$

to the lowest excited state. Hence exactly at the transition point, a level crossing occurs and the ground state is triply degenerate, which demonstrates a discontinuous phase transition. It should be noted that the g_1 term is very important here: without it, the ground-state degeneracy at the transition point would be infinitely large in the thermodynamic limit, making it a multicritical point instead of a first-order transition. This is why we need the g_1 term in our specific TCI model.

To identify the Ising phase-transition line, we restore t_1 and apply a different unitary transformation, $(\alpha,\beta)_{2j-1} \rightarrow (-\beta,-\alpha)_{2j-1}$ and $(\alpha,\beta)_{2j} \rightarrow (\beta,\alpha)_{2j}$ for $j \in$ even, to the Hamiltonian in Eq. (1). We then translate it to spin language by performing a Jordan-Wigner (JW) transformation [25]

$$\alpha_j = \prod_{k=1}^{j-1} \sigma_k^x \sigma_j^z, \quad \beta_j = -\prod_{k=1}^{j-1} \sigma_k^x \sigma_j^y, \quad (3)$$

followed by a Kramers-Wannier duality transformation

$$\sigma_j^x = \tau_{j-1}^x \tau_j^x, \quad \sigma_j^z = \prod_{k<j} \tau_k^z. \quad (4)$$

The resulting Hamiltonian takes the form

$$\begin{aligned} H_S = &\sum_{j=1}^{N/2} -t(\tau_{2j-2}^x + \tau_{2j}^x)\tau_{2j-1}^x - t_1(1 + \tau_{2j-2}^x\tau_{2j}^x)\tau_{2j-1}^z \\ &+ \sum_{j=1}^{N/2-1} g(\tau_{2j-2}^x\tau_{2j}^x + \tau_{2j}^x\tau_{2j+2}^x)\tau_{2j-1}^x\tau_{2j+1}^x \\ &- \sum_{j=1}^{N/2-2} g_1(\tau_{2j-2}^x\tau_{2j+2}^x + \tau_{2j}^x\tau_{2j+4}^x)\tau_{2j-1}^x\tau_{2j+3}^x, \quad (5) \end{aligned}$$

where we defined $\tau_0^x = 1$. Clearly, τ^x operators at even sites commute with the Hamiltonian above and thus represent conserved quantities. Inspecting each term in Eq. (5) individually, it is not difficult to establish that the ground state favors the configuration in which the absolute values of the terms inside the parentheses are maximized. For instance, the ground state of the g term would favor $\tau_{2j}^x\tau_{2j+2}^x = 1$ for all j or else $\tau_{2j}^x\tau_{2j+2}^x = -1$ for all j. When considering the whole Hamiltonian, we expect this argument to hold if all four terms favor the same configuration. Indeed such a configuration exists, having $\tau_{2j}^x = 1$ for all j. In this configuration, it is easy to see that the remaining degrees of freedom are described by the Ising metamagnet model well known to support the TCI point [9]. In the special case when t and g_1 are absent, the Hamiltonian becomes simply that of the transverse field Ising model in which the Ising phase transition occurs exactly at $t_1 = g$. With finite g_1, the transition point is expected to move toward a larger t_1 while preserving the Ising universality class.

III. NUMERICAL RESULTS

The analytical arguments advanced in the previous section identified first-order and Ising phase transitions in two special cases, each of which corresponds to a point on one of the coordinate axes in the t-t_1 phase diagram. In the Ising metamagnet model, it is known that a phase-transition line exists that connects these two points, and a TCI point resides

somewhere along this line. On the basis of the above analysis, we expect the same scenario to take place in our fermionic model. To verify the validity of this conjecture and to locate the TCI point, we performed extensive numerical analysis of the model defined by Eq. (1). Using the density-matrix renormalization-group (DMRG) technique, we located the phase-transition line and we computed the central charge along the line. In the DMRG computations, we performed 10–12 sweeps, and the truncation error in each sweep was set to be lower than 10^{-10}. The central charge c has been extracted from the fit to the entanglement entropy $S(n)$ of the ground state according to the relation [45]

$$S(n) = \frac{c}{3} \ln\left[\frac{N}{\pi} \sin\left(\frac{\pi n}{N}\right)\right] + S_0, \quad (6)$$

where N is the system size, n is the subsystem size, and S_0 is a constant. It should be noted that Eq. (6) only works under (anti)periodic boundary conditions. When a phase transition occurs, either first-order or continuous, the central charge shows a peak. For a continuous phase transition the peak tends to a finite value, while it drops to zero in the thermodynamic limit for a first-order phase transition [46]. We could then locate the phase-transition points and identify their types. We note that in the following DMRG computations, antiperiodic boundary conditions are assumed.

As we discussed earlier, the transition point on the t_1 axis should still belong to the Ising universality class when finite g_1 is switched on. Indeed, our DMRG results shown in Fig. 2 demonstrate that the transition in the presence of g_1 is still characterized by Ising CFT with $c = \frac{1}{2}$. Also we found that for $g_1 \leq g$, the critical point t_1^C is approximately linear with g_1, and the slope is estimated to be 1.5. However, this linear relation would fail for large g_1 since the transition point approaches $t_1^C = g_1$ when $g_1/g \rightarrow \infty$, where the system is described by two decoupled Ising chains, as can be seen in Eq. (5). Since the g_1 term preserves the Ising phase transition on axis t_1 and at the same time introduces the first-order transition on axis t, we can thus expect the TCI phase
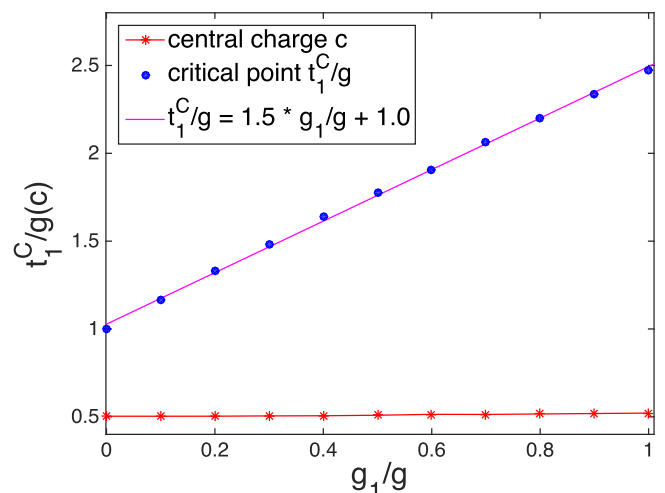

FIG. 2. Phase transition point t_1^C evolves with g_1 in the absence of t and t_2. The system size is $N = 80$.
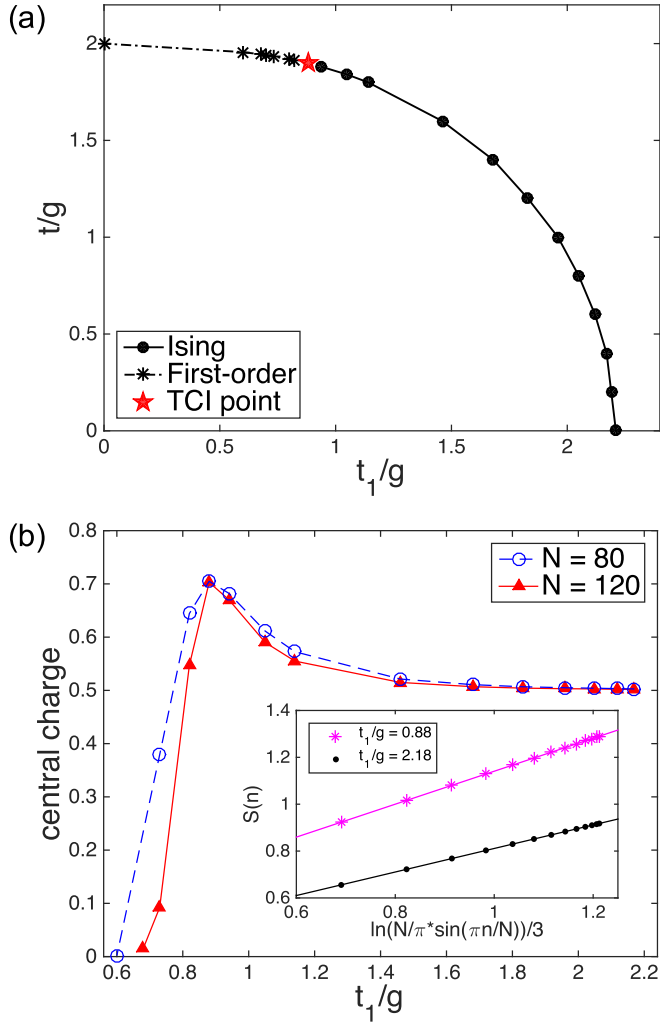
FIG. 3. (a) Phase diagram of the model in the t-t_1 plane (system size $N = 120$) for $t_2 = 0$, and (b) central charge plot along the phase-transition line obtained by DMRG. The inset shows the evolution of entanglement entropy with the length of the subsystem, whose slope gives the central charge, according to Eq. (6). The $t_1/g = 0.88$ line corresponds to the TCI point, with $c = \frac{7}{10}$, and the other line is in the Ising transition regime, with $c = \frac{1}{2}$. In both panels, the interaction strength $g_1/g = 0.8$ is assumed.

transition to occur somewhere in the t-t_1 plane in the presence of finite g_1.

Representative results for generic values of g and g_1 and $t_2 = 0$ are shown in Fig. 3. The central charge plot in Fig. 3(b) clearly demonstrates that a TCI point occurs characterized by a peak with $c = \frac{7}{10}$ that separates the discontinuous portion of the transition line ($c = 0$) from the Ising critical line ($c = \frac{1}{2}$). We note that the TCI points exist in the t-t_1 phase diagram whenever g and g_1 are positive. Different values of these parameters simply alter its position.

Up to now we have not included the t_2 term, which, however, will be present generically in any physical realization of the model. In the following, we argue that weak to moderate values of t_2 (compared to g and g_1) do not qualitatively change the phase diagram shown in Fig. 3(a), and, specifically, the TCI

point remains robustly present. We then present numerical evidence supporting these arguments.

Consider first a case in which $t_2 \gg t, t_1$. The noninteracting Hamiltonian (2) then describes four decoupled critical Majorana chains with only nearest-neighbor hopping. As is known, one such critical chain belongs to the Ising universality class with central charge $c = 1/2$. Four such chains together would trivially add and form a critical system with $c = 2$. To see how the interactions g and g_1 influence the gapless phase, we can transform Eq. (1) into a spin basis. Since in the absence of t and t_1 the system decouples into two identical ladders, we need only to work with one of them. Again we perform a JW transformation on the upper ladder, and the resulting Hamiltonian reads

$$H' = \sum_j -t_2\big(\sigma_j^z \sigma_{j+1}^z + \sigma_j^y \sigma_{j+1}^y\big) - g\sigma_j^x \sigma_{j+1}^x - g_1 \sigma_j^x \sigma_{j+2}^x, \quad (7)$$

which describes the spin-$\frac{1}{2}$ Heisenberg XXZ model with next-nearest-neighbor interactions. To obtain Eq. (7), we have applied a unitary rotation $\sigma_j^z \to -\sigma_j^y$ and $\sigma_j^y \to \sigma_j^z$ for $j \in$ odd, and the lattice index was relabeled since only the upper ladder is considered. In the absence of g_1, the XXZ model shown in Eq. (7) is exactly solvable [47,48], and it is well known that a transition occurs when t_2 increases to $t_2 = g$, at which point the system transits from a ferromagnetic phase to a gapless phase. Turning on finite g_1 is expected to move the transition point toward a larger t_2, since g_1 enhances the ferromagnetic order favored by the g term [49]. We can imagine that in the t-t_1 phase diagram, the ferromagnetic phase would disappear when t_2 exceeds this transition point, and only gapped phases are left since nonzero t and t_1 would gap out the t_2-dominated gapless phase. We thus conclude that in order to preserve the topology of the phase diagram indicated in Fig. 3(a), t_2 must not exceed the interaction parameters g and g_1. Otherwise, no TCI transition shall exist.

To investigate the stability of the TCI point when the t_2 term is weak, we actually only need to focus on the two special cases of the model defined by $t_1 = 0$ and $t = 0$. If the first-order and Ising transitions persist, we can expect the transition line connecting them to still exist and the TCI point thus to survive.

In the first case, a first-order transition occurs at $t = 2g$ in the absence of t_1. Since t_2 favors a gapless phase, one can expect increasing t_2 to drive the first-order transition toward a continuous one. However, for small t_2, the transition can still be discontinuous, considering that the finite gap in the first-order transition point cannot be closed by an arbitrarily weak t_2. As indicated in Fig. 4(a), the first-order transition point indeed continues moving toward small t with the increase of t_2, until in the vicinity of $t = 0$ the transition becomes continuous, characterized by $c = 2$. The same scenario unfolds in the second case, where an Ising transition occurs at $t_1 = t_1^C(g, g_1)$ in the absence of t and t_2. By turning on finite t_2, the critical point moves while still being of Ising type, as is shown in Fig. 4(b). We can thus expect the TCI point to still exist when t_2 is relatively small. This is demonstrated in Fig. 5 by explicit computation of the phase diagram for $t_2 = 0.2$.

To reach the TCI transition point in the setup of Fig. 1, therefore, we require the amplitude of the tunneling terms to be comparable with that of the four-fermion interaction
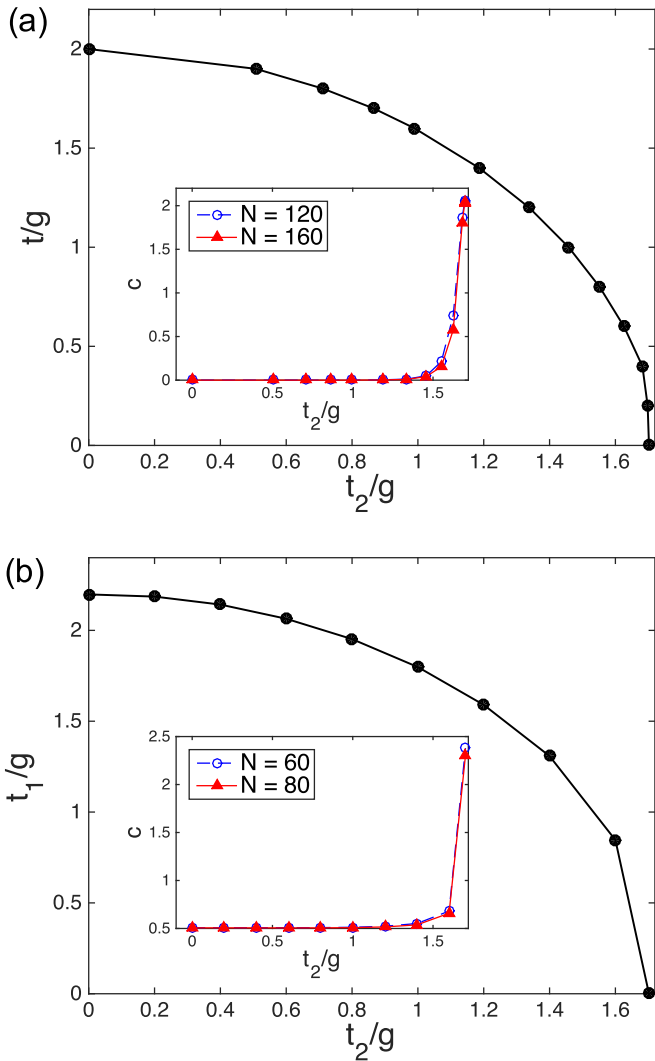
FIG. 4. Influence of t_2 on the first-order and Ising transitions in two special cases ($t_1 = 0$ for the upper panel and $t = 0$ for the lower panel). As before, $g_1/g = 0.8$. The small t_2 term does not affect the transition property, as discussed in the text. The system size is $N = 160$ for the phase diagram in (a) and $N = 80$ for that in (b).
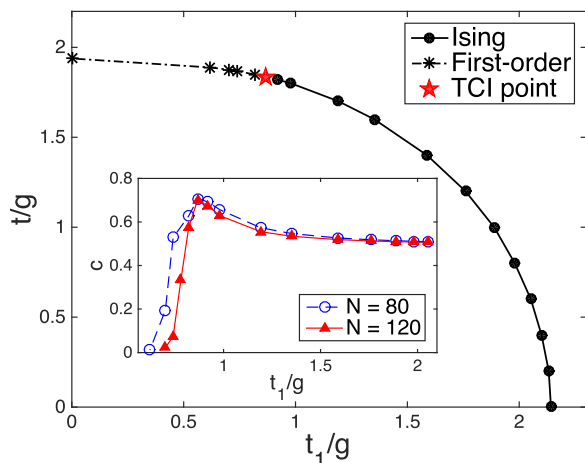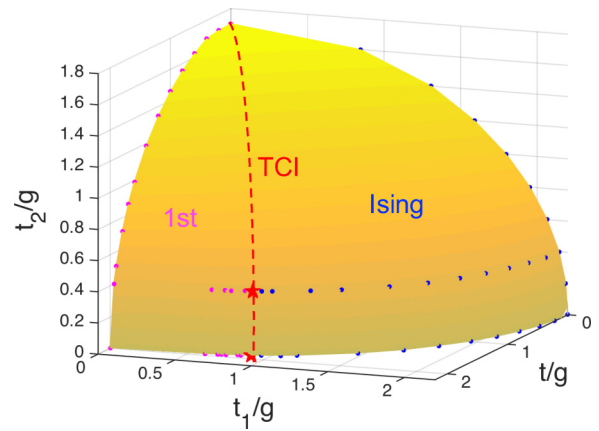

FIG. 6. Phase diagram in (t, t_1, t_2) space. The surface defining the phase transition has been constructed by extrapolating the DMRG results obtained in various limiting cases (shown by blue and magenta dots). The red (dashed) curve represents the approximate position of the TCI phase transition line, which separates the Ising and first-order phase transitions on the phase-transition surface shown in yellow. The TCI points obtained from DMRG are marked by red stars.

terms, a regime of weak to intermediate coupling. The coupling between the upper and lower ladder does not have to be strong compared to the intraladder hopping, as can be seen from Fig. 3(a). Also, we require that the bilinear coupling along the ladder (t_2 term) is comparable to or weaker than the interaction strength.

Figure 6 summarizes our main results. It shows the phase transition surface in the 3D phase diagram spanned by couplings (t, t_1, t_2). The surface consists of the Ising and first-order transition regions separated by a line of TCI points. When t_2 is large enough, the phase-transition line in the (t, t_1) plane shrinks to a point on the t_2 axis that represents a gapless phase, and the TCI point therefore disappears.

IV. SUMMARY AND DISCUSSION

To conclude, we constructed and analyzed a fermionic model with local interactions defined in a two-ladder Majorana lattice, which could be realized in a vortex lattice formed on two parallel surfaces of a proximitized topological insulator film. We established a connection (in a certain limit) between the low-energy sector of our model and an Ising metamagnet spin model well known to support the tricritical Ising point. We have numerically verified the existence of the TCI point in our fermionic model and demonstrated that it occurs in the regime of weak to moderate interaction strength.

To reach the TCI point, two model parameters must be independently tuned, similar to the spin models where the TCI point is known to occur [7–9]. While such a tuning is unlikely to be practical in a spin system (since the coupling constants are typically fixed by the material parameters), it is conceivable, at least in principle, to do this in our model when realized as described above. Here, three quantities at least can be independently controlled: the topological insulator thickness d (by fabrication), its chemical potential μ (by crystal chemistry and gating), and the applied magnetic field B. These three quantities have a very different effect

FIG. 5. Phase diagram ($N = 120$) for nonzero $t_2/g = 0.4$ and $g_1/g = 0.8$. The TCI phase transition is stable against the inclusion of small t_2 except that the position of the TCI point is slightly changed.

on the system parameters: thickness d, for instance, affects predominantly the tunneling amplitude t_1, while the chemical potential influences mostly t and t_2. Magnetic field in turn affects all parameters except t_1. Therefore, by judicious choice of these inputs, one could conceivably locate the transition line present, e.g., in the t-t_1 plane and then move along the line to reach the TCI point. As suggested in Refs. [28,29], various phases and phase transitions can then be probed by tunneling (using a scanning tunneling microscope, for instance) into the zero-mode states in the vortex cores where the tunneling conductance $G(V) = dI/dV$ exhibits a characteristic voltage dependence. For instance, gapped phases of the model would show exponentially activated behavior while Ising and TCI points exhibit power law $G \sim |V|^\alpha$ with $\alpha = 0, 2/5$, respectively. Supersymmetry will be most easily observable on the first-order transition line in the close vicinity of the TCI point. Here it implies the existence of fermionic and bosonic excitations at the same energies. Fermionic excitations can be probed by an ordinary single-electron tunneling while bosonic excitations could be probed by pair tunneling with a superconducting tip [28,29].

Other routes to the TCI point and the associated super-symmetry starting from Majorana fermions are possible and present an interesting subject for future research. One such approach would be to start from an SO(7) CFT, realized in a cluster spin model [50] or using seven decoupled critical Majorana chains, and adding Sugawara-type current-current interactions with a G_2 symmetry (here G_2 refers to the exceptional Lie algebra). This should gap out the primary fields of the G_2 CFT (central charge $\frac{14}{5}$) and leave behind the coset SO(7)/G_2 with central charge $\frac{7}{2} - \frac{14}{5} = \frac{7}{10}$, which likely corresponds to TCI CFT.

We close by noting that ingredients necessary to start exploring various interacting models with Majorana zero modes, including the one introduced in this work, are currently in place. Superconducting order has been induced in topological insulator surfaces by multiple groups and in several different materials [51–59]. The ability to tune the chemical potential to the vicinity of the Dirac point, required to bring in the regime with significant interaction strength, has also been demonstrated [55–57]. More recently, individual vortices have been imaged in these systems [58], and spectroscopic evidence indicative of MZMs in the cores of vortices has been reported [60]. The current proposal requires inducing superconducting order on two surfaces of a topological insulator film, which presents an additional experimental challenge. The rapid progress the field has been experiencing suggests that this challenge can be met in the not too distant future.

[1] M. Henkel, *Conformal Invariance and Critical Phenomena* (Springer, New York, 1999).

[2] P. Francesco, P. Mathieu, and D. Sénéchal, *Conformal Field Theory* (Springer, New York, 1997).

[3] S. P. Martin, arXiv:hep-ph/9709356.

[4] D. Friedan, Z. Qiu, and S. Shenker, Phys. Rev. Lett. **52**, 1575 (1984).

[5] D. Friedan, Z. Qiu, and S. Shenker, Phys. Lett. B **151**, 37 (1985).

[6] Z. Qiu, Nucl. Phys. B **270**, 205 (1986).

[7] M. Blume, Phys. Rev. **141**, 517 (1966).

[8] H. Capel, Physica **32**, 966 (1966).

[9] M. Henkel, J. Phys. A **23**, 4369 (1990).

[10] F. Wilczek, Nat. Phys. **5**, 614 (2009).

[11] J. Alicea, Rep. Prog. Phys. **75**, 076501 (2012).

[12] C. W. J. Beenakker, Annu. Rev. Condens. Matter Phys. **4**, 113 (2013).

[13] T. D. Stanescu and S. Tewari, J. Phys. Condens. Matter **25**, 233201 (2013).

[14] S. R. Elliott and M. Franz, Rev. Mod. Phys. **87**, 137 (2015).

[15] E. M. Stoudenmire, J. Alicea, O. A. Starykh, and M. P. A. Fisher, Phys. Rev. B **84**, 014503 (2011).

[16] S. Gangadharaiah, B. Braunecker, P. Simon, and D. Loss, Phys. Rev. Lett. **107**, 036801 (2011).

[17] E. Sela, A. Altland, and A. Rosch, Phys. Rev. B **84**, 085114 (2011).

[18] F. Hassler and D. Schuricht, New J. Phys. **14**, 125018 (2012).

[19] H. Katsura, D. Schuricht, and M. Takahashi, Phys. Rev. B **92**, 115137 (2015).

[20] R. Thomale, S. Rachel, and P. Schmitteckert, Phys. Rev. B **88**, 161103 (2013).

[21] Y.-H. Chan, C.-K. Chiu, and K. Sun, Phys. Rev. B **92**, 104514 (2015).

[22] M. Cheng and H.-H. Tu, Phys. Rev. B **84**, 094503 (2011).

[23] F. Iemini, L. Mazza, D. Rossini, R. Fazio, and S. Diehl, Phys. Rev. Lett. **115**, 156402 (2015).

[24] N. Lang and H. P. Büchler, Phys. Rev. B **92**, 041118 (2015).

[25] P. Fendley, J. Stat. Mech.: Theor. Exp. (2012) P11020.

[26] A. Y. Kitaev, Phys. Usp. **44**, 131 (2001).

[27] T. Grover, D. N. Sheng, and A. Vishwanath, Science **344**, 280 (2014).

[28] A. Rahmani, X. Zhu, M. Franz, and I. Affleck, Phys. Rev. Lett. **115**, 166401 (2015).

[29] A. Rahmani, X. Zhu, M. Franz, and I. Affleck, Phys. Rev. B **92**, 235123 (2015).

[30] V. Mourik, K. Zuo, S. M. Frolov, S. R. Plissard, E. P. A. M. Bakkers, and L. P. Kouwenhoven, Science **336**, 1003 (2012).

[31] A. Das, Y. Ronen, Y. Most, Y. Oreg, M. Heiblum, and H. Shtrikman, Nat. Phys. **8**, 887 (2012).

[32] M. T. Deng, C. L. Yu, G. Y. Huang, M. Larsson, P. Caroff, and H. Q. Xu, Nano Lett. **12**, 6414 (2012).

[33] L. P. Rokhinson, X. Liu, and J. K. Furdyna, Nat. Phys. **8**, 795 (2012).

[34] A. D. K. Finck, D. J. Van Harlingen, P. K. Mohseni, K. Jung, and X. Li, Phys. Rev. Lett. **110**, 126406 (2013).

[35] S. Nadj-Perge, I. K. Drozdov, J. Li, H. Chen, S. Jeon, J. Seo, A. H. MacDonald, B. A. Bernevig, and A. Yazdani, Science **346**, 602 (2014).

[36] L. Fu and C. L. Kane, Phys. Rev. Lett. **100**, 096407 (2008).

[37] C.-K. Chiu, D. I. Pikulin, and M. Franz, Phys. Rev. B **91**, 165402 (2015).

[38] D. I. Pikulin, C.-K. Chiu, X. Zhu, and M. Franz, Phys. Rev. B **92**, 075438 (2015).

[39] A. Milsted, L. Seabra, I. C. Fulga, C. W. J. Beenakker, and E. Cobanera, Phys. Rev. B **92**, 085139 (2015).

[40] S. Vijay, T. H. Hsieh, and L. Fu, Phys. Rev. X **5**, 041038 (2015).

[41] T. Liu and M. Franz, Phys. Rev. B **92**, 134519 (2015).

[42] J. M. Murray and O. Vafek, Phys. Rev. B **92**, 134520 (2015).

[43] J. C. Y. Teo and C. L. Kane, Phys. Rev. B **82**, 115120 (2010).

[44] E. Grosfeld and A. Stern, Phys. Rev. B **73**, 201303 (2006).

[45] P. Calabrese and J. Cardy, J. Stat. Mech. (2004) P06002.

[46] J. C. Xavier and F. C. Alcaraz, Phys. Rev. B **84**, 094410 (2011).

[47] C. N. Yang and C. P. Yang, Phys. Rev. **150**, 321 (1966).

[48] F. D. M. Haldane, Phys. Rev. Lett. **45**, 1358 (1980).

[49] S. Hirata and K. Nomura, Phys. Rev. B **61**, 9453 (2000).

[50] V. Lahtinen and E. Ardonne, Phys. Rev. Lett. **115**, 237203 (2015).

[51] G. Koren, T. Kirzhner, E. Lahoud, K. B. Chashka, and A. Kanigel, Phys. Rev. B **84**, 224521 (2011).

[52] B. Sacepe, J. B. Oostinga, J. Li, A. Ubaldini, N. J. G. Couto, E.Giannini, and A. F. Morpurgo, Nat. Commun. **2**, 575 (2011).

[53] F. Qu, F. Yang, J. Shen, Y. Ding, J. Chen, Z. Ji, G. Liu, J. Fan, X. Jing, C. Yang, and L. Lu, Sci. Rep. **2**, 339 (2012).

[54] J. R. Williams, A. J. Bestwick, P. Gallagher, S. S. Hong, Y. Cui, A. S. Bleich, J. G. Analytis, I. R. Fisher, and D. Goldhaber-Gordon, Phys. Rev. Lett. **109**, 056803 (2012).

[55] S. Cho, B. Dellabetta, A. Yang, J. Schneeloch, Z. Xu, T. Valla, G. Gu, M. J. Gilbert, and N. Mason, Nat. Commun. **4**, 1689 (2013).

[56] S.-Y. Xu, N. Alidoust, I. Belopolski, A. Richardella, C. Liu, M. Neupane, G. Bian, S.-H. Huang, R. Sankar, C. Fang, B. Dellabetta, W. Dai, Q. Li, M. J. Gilbert, F. Chou, N. Samarth, and M. Z. Hasan, Nat. Phys. **10**, 943 (2014).

[57] L. Zhao, H. Deng, I. Korzhovska, J. Secor, M. Begliarbekov, Z. Chen, E. Andrade, E. Rosenthal, A. Pasupathy, V. Oganesyan, and L. Krusin-Elbaum, Nature Comm. **6**, 8279 (2015).

[58] J.-P. Xu, C. Liu, M.-X. Wang, J. Ge, Z.-L. Liu, X. Yang, Y. Chen, Y. Liu, Z.-A. Xu, C.-L. Gao, D. Qian, F.-C. Zhang, and J.-F. Jia, Phys. Rev. Lett. **112**, 217001 (2014).

[59] A. D. K. Finck, C. Kurter, Y. S. Hor, and D. J. Van Harlingen, Phys. Rev. X **4**, 041022 (2014).

[60] J.-P. Xu, M.-X. Wang, Z. L. Liu, J.-F. Ge, X. Yang, C. Liu, Z. A. Xu, D. Guan, C. L. Gao, D. Qian, Y. Liu, Q.-H. Wang, F.-C. Zhang, Q.-K. Xue, and J.-F. Jia, Phys. Rev. Lett. **114**, 017001 (2015).